Vol 1 (1) (2020)1851-0551

Measurement, Control, and Automation

Website: https:// mca-journal.org

ISSN 1859-0551

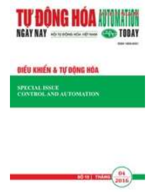

Optimal calculation of Plate Fin Heat Sinks for RRU LTE 4G

Dinh Bui Minh [1] and Vuong Dang Quoc[1]

[1]*School of Electrical Engineering, Hanoi University of Scienece and Technology*
E-mail: dinh.buiminh@hust.edu.vn and vuong.dangquoc@hust.edu.vn

Abstract

Remote Radio Unit RRU 4G LTE Heatsink systems works based on the natural convection cooling, usually working outdoors in the harsh conditions of temperature, humidity, hoarfrost. However, this device has some advantages, i.e., low cost, high reliability. Its main drawback is a relatively low heat transfer. Therefore, in order to reinforce a capablity of heat transfer, the optimal calculation of Plate Fin Heat Sinks for RRU LTE 4G to reduce power losses plays an important role and is always topical subjects for researchers and designers. In this study, the paper uses a real model of 4G RRU device with the capacity of 2x40W and 2x60W. Model is made of parallel heat sinks and is naturally cooled.

Keywords: *Radio transmitter, transceivers, power amplifiers, receivers, 4G mobile communication*

Tóm tắt

Hệ thống tản nhiệt thiết bị thu phát viễn thông RRU 4G làm việc dựa trên mô hình tản nhiệt đối lưu tự nhiên, thường làm việc ngoài trời trong điều kiện khắc nghiệt về nhiệt độ, độ ẩm, sương muối. Tuy nhiên, thiết bị có nhiều ưu điểm như giá thành gia công sản xuất thấp và độ tin cậy cao, nhược điểm duy nhất là khả năng truyền nhiệt thấp. Do đó, để tăng cường khả năng truyên nhiệt, việc tính toán tối ưu kích thước gân cánh tản nhiệt để đảm bảo tiêu tán công suất tản nhiệt ra ngoài môi trường đóng vai trò rất quan trọng và luôn mang tính thời sự với các nhà khoa học và nhà thiết kế. Trong nghiên cứu này, bài báo áp dụng cho mô hình thực của thiết bị RRU 4G có công suất 2x40W và 2x60W. Mô hình có cấu tạo từ các tấm tản nhiệt song song và được làm mát tự nhiên..

1. Introduction

Nowadays, the application of LTE 4G for carrying RF/microwave circuit design with high frequencies plays an important role in reality [1]. Thus, the optimal computation of Plate Fin Heat Sinks for RRU LTE in order to reduce power loss density due to higher frequencies and higher powers is always mandatory for researchers and designers. [1]- [6]. In this paper, the output of power amplifier (PA) in RF/microwave circuits is from 2x40 W to 2x60W with efficiency of 30 - 40%. Most of input powers will be converted to heating losses [1]-[4]. Total heat losses are about from 240 W to 300 W based on the PA operation modes. So as to adjust the overheat temperature of the PA transistor, the natural convection heat sink is designed to dissipate the heat loss to air in different cases. Consequently, a finite element method (FEM) has been applied to calculate thermal distributions of the RRU housing system and the hotspot of PA base. The thermal dissipation density is maximized to meet RF/microwave performance and size reduction.

The multi-physic analysis has been recently demonstrated that the characterization of wire bonding interconnects and the printed circuit board laminate materials are very important [2]-[4].

The aim of this paper is to present a modelling of thermal problems that include a full-wave electromagnetic and a transient thermal simulation via an process iteration. The calculation is performed by the FEM due to its unmatched capabilities in complicated geometries and materials [4]. The analytical calculation is applied to different heat sink profiles and the finite element simulations are setup to performance thermal management.

Temperature measurements are performed to illustrate the theory of developed method. The obtained thermal performance is then used to the thermal resistance of different RRU heatsink. This paper will calculate an optimal aluminum thickness of fin heatsink of RRU housing to minimum material cost.

2. Analytical Model

The analytical model of the natural convection heatsink investigated by Elenbass is depicted in Figure 1. This natural convection between isothermal parallel vertical The dimension of the natural convection heat sink for RRU made by aluminum is the 425 x 320 x 140 (mm^3). The heat sink is set to close to the power amplifier unit in RRU. In addition, the natural convection heat sink is the cover of RRU [7], [8]. Analytical model of heatsink fins is shown in Figure 2.

The thermal problems (i.e., heat transfer performance, thermal resistance, and thermal conductivity of natural

Received: 25 May 2020; Accepted: 10 June 2020; Published: 26 September 2020.

convection cooling) with different geometries are studied in this paper.

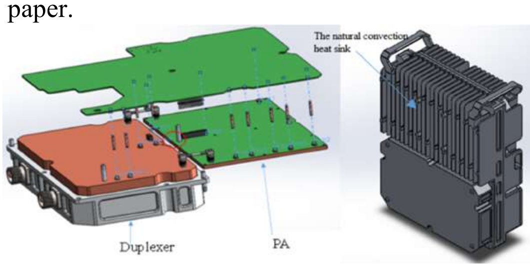

Figure 1: Schematic of the natural convection heatsink.

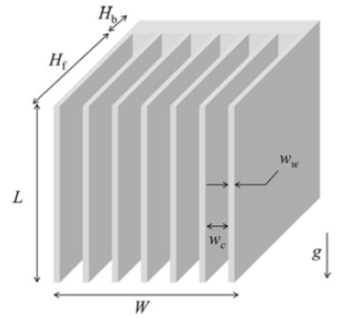

Figure 2: Input parameters of heatsink [2].

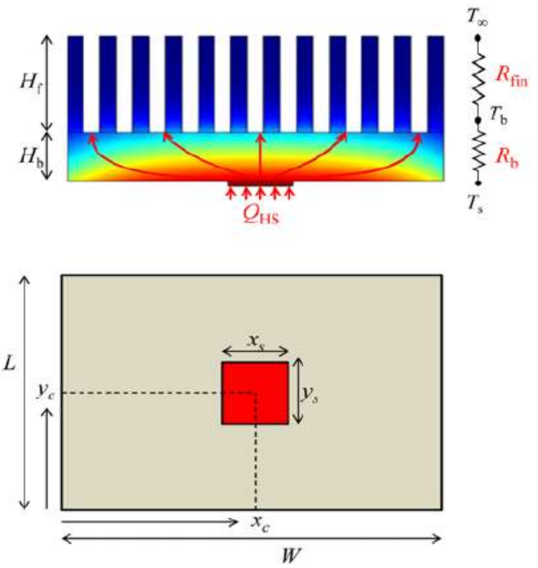

Figure 3: The heat sinks with heat source.

The heat flow via a natural convection is expressed [9], [10]

$$Q_{HS} = n_{fin}.Q_{fin} + h_b A_b \theta_b + Q_{rad} \qquad (1)$$

$$n_{fin} = \frac{W+w_c}{w_c+w_w},\ A_b = Lw_c(n_{fin}-1),$$

$$Q_{fin} = h_{fin}A_{fin}\theta_b, \qquad (2a\text{-}b\text{-}c)$$

where n_{fin} is the fin numbers, Q_{fin} is the heat dissipated heat in each fin, h_b is heat transfer coefficient in each fin, A_b is the heat sink surface area in each fin, θ_b is the differential temperature between ambient temperature and fin, Q_{rad} is the radiation heat transfer. Geometric parameters (W, w_c and w_w) are given in Figure 3.

The parameter Afin in (2 c) is gives

$$A_{fin} = 2\left(LH_f + H_f w_w + \frac{Lw_w}{2}\right), \qquad (3)$$

where L, H_f and H_b are geometric parameters are also given in Figure 3. The external and internal heat transfer coefficient for a single fin are given respectively

$$h_b = 0.59Ra_b^{0.25}\frac{k_f}{L}, \quad h_{fin} = Nu_{fin}\frac{k_f}{w_c}, \qquad (4a\text{-}b)$$

where k_f represents the thermal factor in air and Nufin is the nusselt standard of the heatsink.

$$Nu_{fin} = \left[\frac{576}{(\eta_{fin}El)^2} + \frac{2.873}{(\eta_{fin}El)^{\frac{1}{2}}}\right]^{\frac{-1}{2}}. \qquad (5)$$

The Rayleigh number (Rab) and Elenbaas number El in (5) are respectively defined as

$$El = \frac{g\beta\theta_b w_c^4}{v_f\alpha_f L}, \qquad Ra_b = \frac{g\beta\theta_b L^3}{v_f\alpha_f}, \qquad (6a-b)$$

where v_f and α_f are the viscosities and the thermal conductivities of the cooling medium air, respectively.

The radiation of heat transfer coefficient Q_{rad} is estimated by

$$Q_{rad} = \sigma\varepsilon_{eff}LW(T_b^4 - T_\infty^4), \qquad (7)$$

where ε_{eff} is the emissivity of the solid made of the aluminum, σ is the Boltzmann constant and L.W is the heat surface sink without including the shape of the channels. When the surface radiation coefficient Qrad is 0.8, the emissivity is defined [9], [10]

$$\varepsilon_{eff} = \left[-0.2 - 3.369\,exp\left(-\frac{L}{0.929H_f}\right)\right] exp\left(-\frac{H_f}{2s}\right) + 1.12 + 3.004\,exp\left(-\frac{L}{1.526H_f}\right). \qquad (8)$$

The thermal resistence appears when heat flow transfers from the narrow area to the larger area. The thermal resistence is given by

$$R_{fin} = \frac{\theta_b}{Q_{HS}}. \qquad (9)$$

The temperature at any location θ(x, y, z) distributed in plate is computed [1]-[6]. It can be expressed as

$$\theta(x,y,z) = A_o + B_o z + \sum_{m=1}^{\infty} cos\,\lambda_m\,x[A_m\,cosh\,\lambda_m\,z + B_m\,sinh\,\lambda_m\,z] + \sum_{n=1}^{\infty} cos\,\delta_n\,x[A_n\,cosh\,\delta_n\,z + B_n\,sinh\,\delta_n\,z] + + \sum_{m=1}^{\infty}\sum_{n=1}^{\infty} cos\,\lambda_m\,x\,cos\,\delta_n\,y[A_{mn}\,cosh\,\beta_{mn}\,z + B_{mn}\,sinh\,\beta_{mn}\,z], \qquad (10)$$

where factors A_m, A_n and A_{mn} are defined as

$$A_m = \frac{2Q_{HS}\left[sin\left(\frac{2x_c+x_s}{2}\right)\lambda_m - sin\left(\frac{2x_c-x_s}{2}\right)\lambda_m\right]}{LWx_s k\lambda_m^2\phi\lambda_m},$$

$$A_n = \frac{2Q_{HS}\left[sin\left(\frac{2y_c+y_s}{2}\right)\delta_n - sin\left(\frac{2y_c-y_s}{2}\right)\delta_n\right]}{LWy_s k\delta_n^2\phi\delta_n},$$

$$A_{mn} = \frac{16Q_{HS}\cos\lambda_m x_c \sin\left(\frac{1}{2}\lambda_m m_s\right)\cos(\delta_n y_c)\sin\left(\frac{1}{2}\delta_n d\right)}{LWx_x y_s k\beta_{mn}\lambda_m\delta_n\phi(\beta_{mn})},$$

with

$$\lambda = \frac{m\pi}{W}, \delta = \frac{n\pi}{L}, \beta = (\lambda^2+\delta^2)^{0.5},$$

$$B_i = -\phi(\zeta)A_i, \qquad (11a-b-c)$$

$$\phi(\zeta) = \frac{\zeta \sinh\zeta H_b + \frac{h_{eff}}{k\cosh\zeta H_b}}{\zeta\cosh\zeta H_b + \frac{h_{eff}}{k\sinh\zeta H_b}}. \qquad (12)$$

The factor ζ in (12) is now replaced by correlated λ, δ, β

$$\begin{aligned}\rightarrow \theta_h = {} & \frac{Q}{LW}\left(\frac{H_b}{k}+\frac{1}{h_{eff}}\right) \\ & + 2\sum_{m=1}^{\infty} A_m \frac{\cos\lambda_m x_c \sin\left(\frac{1}{2}\lambda_m x_s\right)}{\lambda_m x_s} \\ & +2\sum_{n=1}^{\infty} A_n \frac{\cos\delta_n y_c \sin\left(\frac{1}{2}\delta_n y_s\right)}{\delta_n y_s} \\ & +2\sum_{n=1}^{\infty} A_n \frac{\cos\delta_n y_c \sin\left(\frac{1}{2}\delta_n y_s\right)}{\delta_n y_s} \\ & +4\sum_{m=1}^{\infty}\sum_{n=1}^{\infty} A_{mn}\frac{\cos\lambda_m x_c\sin\left(\frac{1}{2}\lambda_m x_s\right)\cos\delta_n y_c \sin\left(\frac{1}{2}\delta_n x_s\right)}{\lambda_m\delta_n x_s y_s}\end{aligned} \qquad (13)$$

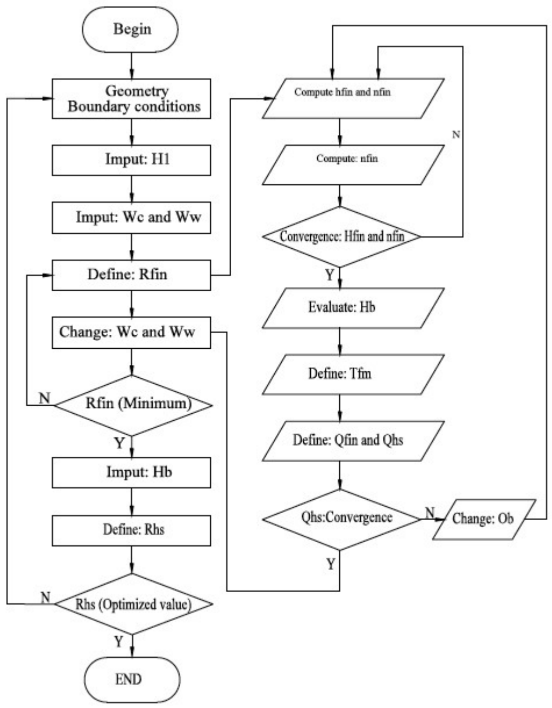

Figure 4: Optimal heatsink fins calculation.

If have many the heat sources, the average value should be computed. Finally, the thermal resistance is given by

$$R_{HS} = \frac{\overline{\theta}_{hea}}{Q_{HS}}. \qquad (14)$$

The factors k and h_{eff} in (12) are thermal conductivity coefficients defined as

$$h_{eff} = \frac{1}{R_{fin}LW}. \qquad (15)$$

The algorithm for computing the thermal conductivity coefficients is presented in Figure 4.

The input parameters for optimal fins are herein Q = 300W, L = 174 mm, W = 380 mm, t_b = 5 mm, b = 12 mm, H = 55 mm. The entropy $\dot{S}_{gen}$ is a function of the fin thickness shown in Figures 5 and 6 [1]-[6]. The Entropy and Resistance is minimum with heatsink thickness of 1.5 mm, however CNC machines can manufacture the heatsink fin from 2mm because of deformation (Fig. 7). The number of fins (n = 32) and the thickness (d = 2mm) are optimal parameters of RRU heatsinks. Those parameters will apply for 3D design by Solid work and NX software

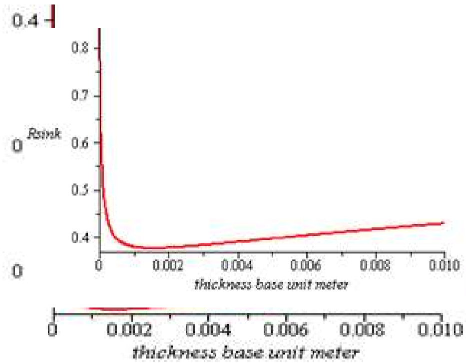

Figure 5: Entropy vs fin thickness [2].
Figure 6: Heatsink resistence and fin thickness [2].

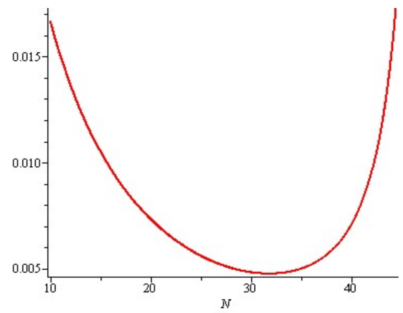

Figure 7: Optimal number of fins [2].

3. Thermal simulation

The 3-D model and material parameters have been loaded in Ansys-Icepack model to determine temperature distributions of the RRU heatsink. The hotspot is located in center of heat source. The maximum temperature must be lower than temperature limit of IC PA transistor, modeling steps is shown in Figure 8.

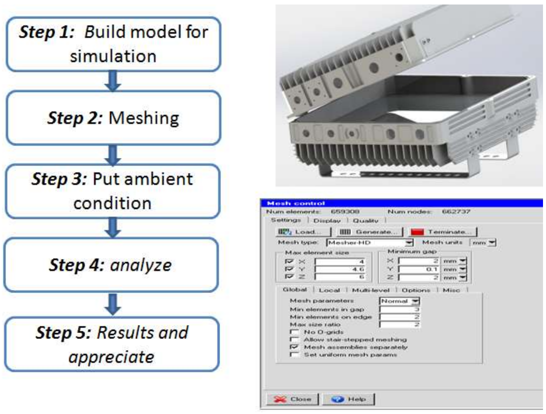

Figure 8: Modeling steps.

Blocks : (18)							
Object			**Material**		**No. of Sides**	**Power**	
Name	**Shape**	**Block type**	**Surface**	**Solid**	**Num Sides Added**	**Total**	**Type**
Cir L.1	Bsplines	Solid	Steel-Oxidised-surface	Al-Extruded	2	6.0 W	constant
Cir L.2	Bsplines	Solid	Steel-Oxidised-surface	Al-Extruded	2	6.0 W	constant
Cover	Bsplines	Solid	Steel-Oxidised-surface	Al-Extruded	2		
Cover Dup Band3	Bsplines	Solid	Steel-Oxidised-surface	Al-Extruded	2		
Cover Dup Band3 No2	Bsplines	Solid	Steel-Oxidised-surface	Al-Extruded	2		
Driver.1	Bsplines	Solid	Steel-Oxidised-surface	Al-Extruded	2	7.0 W	constant
Driver.2	Bsplines	Solid	Steel-Oxidised-surface	Al-Extruded	2	7.0 W	constant
FPGA	Bsplines	Solid	Steel-Oxidised-surface	Al-Extruded	2	8.5 W	constant
Housing 4G Band3 20180416	Bsplines	Solid	{Paint-Al surface}	{Aluminum 6061-T6}	2	24.0 W	constant
Other IC.1	Bsplines	Solid	Steel-Oxidised-surface	Al-Extruded	2	2.0 W	constant
Other IC.2	Bsplines	Solid	Steel-Oxidised-surface	Al-Extruded	2	2.0 W	constant
PW IC.1	Bsplines	Solid	Steel-Oxidised-surface	Al-Extruded	2	3.0 W	constant
PW IC.2	Bsplines	Solid	Steel-Oxidised-surface	Al-Extruded	2	3.0 W	constant
PW IC.3	Bsplines	Solid	Steel-Oxidised-surface	Al-Extruded	2	3.0 W	constant
PW Module	Bsplines	Solid	Steel-Oxidised-surface	Al-Extruded	2	25.0 W	constant
RAM	Bsplines	Solid	Steel-Oxidised-surface	Al-Extruded	2	2.0 W	constant
TR1	Bsplines	Solid	Steel-Oxidised-surface	Al-Extruded	2	70.0 W	constant
TR2	Bsplines	Solid	Steel-Oxidised-surface	Al-Extruded	2	70.0 W	constant

Figure 9: Material properties.

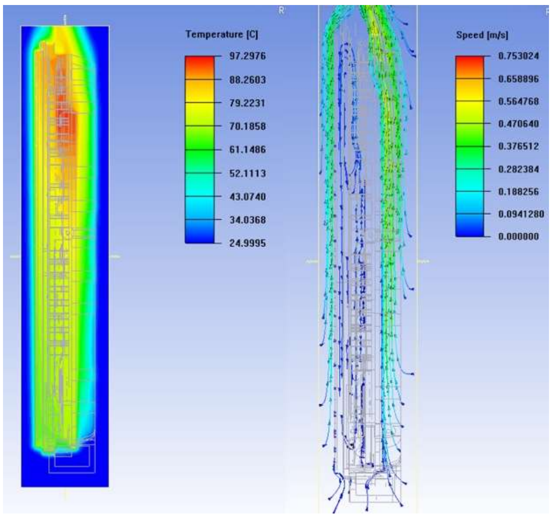

Figure 10: Thermal simulation results.

Material properties of the thermal conduction and heat losses are inputs of the finite element model. The total heat source is form 260W to 300W at the ambient temperature of 250C and natural convection (Fig. 9).

Aluminum conduction AL6061 of 171 W/m.K has installed and applied for the thermal model. The maximum temperature of RRU heatsink is 970C being lower than the temperature capacity of ICS inside the RRU housing (Fig. 10) with using the nemann boundary condition. In order to evaluate the simulation results, an hardware setup has built.

4. Experiment results

The experimental setup includes heatsink, heat source and data acquisition to record temperature values with time sample of 30 second.

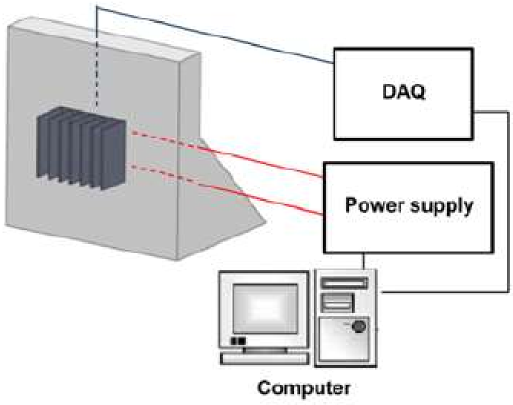

Figure 11: Schematic of experimental setup.

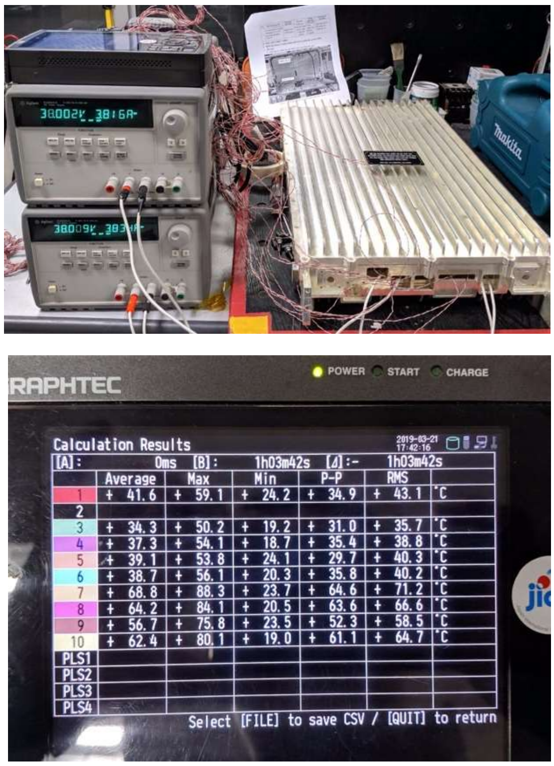

Figure 12: Temperature sensors in RRU housing.

The modelling of the experimental setup is presented in Figure 11, that consists of the power amplifier of RRU heatsink of 240-300W (heat source), data acquisition with 16 chanels for 16 measure points, and desktop PC. The heat transfer plate where the heat source following is inserted to the sidewall of heating block, and the input power value is performed by the multimeter.

The input power for the RRU heat source is 38V*3.8A=245W and the temperature in PCB and IC base and heatsink fin are record by data acquisition and PC in Figure 12 (top). According to IEC experimental test, the maximum temperature is kept in 30 minutes.

Temperature results are recorded by the data acquisition in directorate for standards, metrology and quality (Quatest I), Viet Nam (Fig. 12, *bottom*). After 3 hour workings, the maximum temperature reaches 990^0C checked to be very close to simulation results of 97^0C degree.

5. Conclusions

The achieved results from the thermal modeling are verified to be similar to the results obtained from the measured modeling. The results have shown that the power loss distribution in a wide range. This is illustrated that there is a good validation to use an adapted method to effectively compute and design the natural convection heat sinks of the RRU heatsink. The analytical optimization design points out a capacity of computed heat transfer sinks that is compared to available profiles. In addition, the optimization design also shows the plate area utilized effectively. Hence, power modules is not the preferred selection, but discretization of semiconductors, where the power circuit can design an optimal plate area. The obtained results are computed in the frequency domain.

References

[1] A. Bejan and S. Lorente *Thermodynamic optimization of flow geometry in mechanical and civil engineering*. J. Non-Equilib. Thermodyn., vol. 26, 2001, pp. 305-354.

[2] A. Bejan, G. Tsataronis, and K. Moran *Thermal Design and Optimization*. New York: Wiley, 1996.

[3] A. Bejan *Entropy Generation Minimization*. Boca Raton, FL: CRCPress, 1996.

[4] *Advanced Engineering Thermodynamics*. New York: Wiley,1998.

[5] A. D. Kraus and A. Bar-Cohen *Design and Analysis of Heat Sinks*. New York: Wiley, 1995.

[6] W. M. Kays and A. L. London *Compact Heat Exchangers*. New York: McGraw-Hill, 1984.

[7] Y. S. Muzychka and M. M. Yovanovich *Modeling friction factors in non-circular ducts for developing laminar flow* in Proc. 2nd AIAA. Theoretical Fluid Mech. Meeting, Albuquerque, NM, June 15–18, 1998.

[8] J. Rabkowski, D. Peftitsis, and H.-P. Nee *Design steps towards a 40-kVA SiC JFET inverter with natural-convection cooling and an efficiency exceeding 99.5%*. IEEE Transactions on Industry Applications, vol. 49, no. 4, pp. 1589–1598, Jul./Aug, 2013.

[9] R. Garcia, R. Liu, and V. Lee *Optimal design for natural convection-cooled rectifiers*. IEEE 18th International Telecommunications Energy Conference, INTELEC ’96, Boston, Oct. 1996, pp. 813–822.

[10] T. K¨oneke, A. Mertens, D. Domes, and P. Kanschat *Highly efficient 12kVA inverter with natural convection cooling using SiC switches*. In PCIM Europe, Nuremberg, Germany, May 2011, pp. 1189–1194.